Determination of the Local Chemical Structure of Graphene Oxide and Reduced Graphene Oxide

By *Kris Erickson, Rolf Erni, Zonghoon Lee, Nasim Alem, Will Gannett,* and *Alex Zettl**

Although the unique electronic and mechanical properties of graphene suggest numerous intriguing applications, the requisite large-scale direct synthesis and solution-based handling have proven difficult.[1,2] It has been suggested that a functionalized form of graphene, graphene oxide (GO), could provide a solution-friendly route to facile, high-throughput graphene manipulation.[2] For such a route to be viable, however, GO must be convertible back to graphene, ostensibly via chemical reduction and thermal annealing. Unfortunately, transport measurements indicate that the reconstituted material, reduced and annealed graphene oxide (raGO), has electrical conductivity orders of magnitude lower than that of graphene.[2,3] This raises the question: can oxidized graphene be effectively converted back to graphene, and if not, what can it be converted to?

Central to this question are the detailed atomic structures of GO and raGO, which, despite their importance, remain largely unknown.[4] We present here ultra-high-resolution transmission electron microscopy (TEM) images and dynamics studies of suspended sheets of graphene, GO, and raGO, obtained using aberration-corrected instrumentation. It should be noted that both the label GO and raGO (also referred to as "chemically converted graphene")[5] refer to a wide variety of materials with the properties of each material being largely dependent upon the particular synthetic route employed. This study presents one particular synthetic method for GO and raGO. Among the various methods possible for synthesizing GO and raGO, we followed methods which have yielded the highest reported final conductivities, as this material would be most suitable as a potential graphene alternative.[2,6–11] The local and global structure and stability of GO and raGO are revealed. We find that the raGO material under study is greatly structurally dissimilar to graphene, being unstable under significant electron beam

exposure and having remaining functionalities, and this material is generally not a suitable graphene replacement. Furthermore, our studies greatly help to resolve the theoretical debate about the structure of the important intermediate material GO.

Suspended specimens of pure graphene were prepared using previously described methods.[12] GO was produced via a modified Hummers,[8,13] method and drop cast onto lacey carbon TEM grids. For raGO specimens, GO-containing grids were reduced in a hydrazine atmosphere and then slowly heated to 550 °C under flowing N_2. Initial microscopy with a HR-TEM (JEOL 2010) at 100 kV confirmed the layer number for suspended specimens via electron diffraction (Supporting Information Figure S1).[14,15] Atomic resolution microscopy images were obtained with the TEAM 0.5 TEM (a monochromated aberration-corrected instrument operated at 80 keV). TEAM 0.5 imaging was performed in a high vacuum environment ($<10^{-7}$ mbar), and the electron monochromator was adjusted to enable an energy spread of the electron beam of less than 0.2 eV. The aberration corrector was fine tuned to obtain a third-order spherical aberration of −14 μm, which in consideration of the positive fifth-order aberration of 5.2 mm yielded an optimal phase contrast for a slight positive defocus of +8 nm down to the information limit of 0.08 nm at 80 kV.[3] The resulting electron dose is approximately $2.8*10^6$ electrons/(sec*nm²). Details of the microscope configuration can be found elsewhere.[16,17] Grids were briefly (8 min.) placed on a hot plate at 140 °C to facilitate ambient hydrocarbon desorption.

Figure 1A–C show high resolution TEM images of suspended monolayer sheets of graphene, GO, and raGO, respectively. Images were processed with an FFT bandpass filter for greater clarity. As is well known,[15] graphene consists of an extended, two dimensional sp^2 bonded carbon "honeycomb" lattice. After heating and additional electron beam exposure, hydrocarbon adsorbates, often seen during TEM imaging,[18] desorb, leaving a pristine graphene sheet (Figure 1A).

Following oxidation of the parent graphene, the resulting GO material (Figure 1B) is found to be highly inhomogeneous with respect to structure. Three major features are present: holes (indicated in blue), graphitic regions (indicated in yellow, as they were for Figure 1A), and high contrast disordered regions (indicated in red), indicating areas of high oxidation, with approximate area percentages of 2%, 16%, and 82%, respectively. Holes form in GO as CO and CO_2 are released during the aggressive oxidation and sheet exfoliation,[19] found here to be usually less than 5 nm². Although some high resolution electron microscopy studies have not reported holes in GO samples,[20] a high resolution aberration corrected electron microscopy study of the reduced form of GO has observed similar holes.[21] Graphitic regions, covering between 1 and 6 nm², indicate incomplete oxidation of the basal plane with the preserved honeycomb

[*]   K. Erickson, Dr. N. Alem, W. Gannett, Prof. A. Zettl
      University of California at Berkeley and, Materials
      Sciences Division
      Lawrence Berkeley National Laboratory
      Berkeley, CA 94720 (USA)
      E-mail: azettl@berkeley.edu

      Dr. R. Erni
      National Center for Electron Microscopy
      Lawrence Berkeley National Laboratory and, Electron Microscopy
      Center, Empa
      Swiss Federal Laboratories for Materials Testing and Research
      Ueberlandstr. 129, CH-8600 Dübendorf (Switzerland)

      Dr. Z. Lee
      National Center for Electron Microscopy
      Lawrence Berkeley National Laboratory
      Berkeley, CA 94720 (USA)
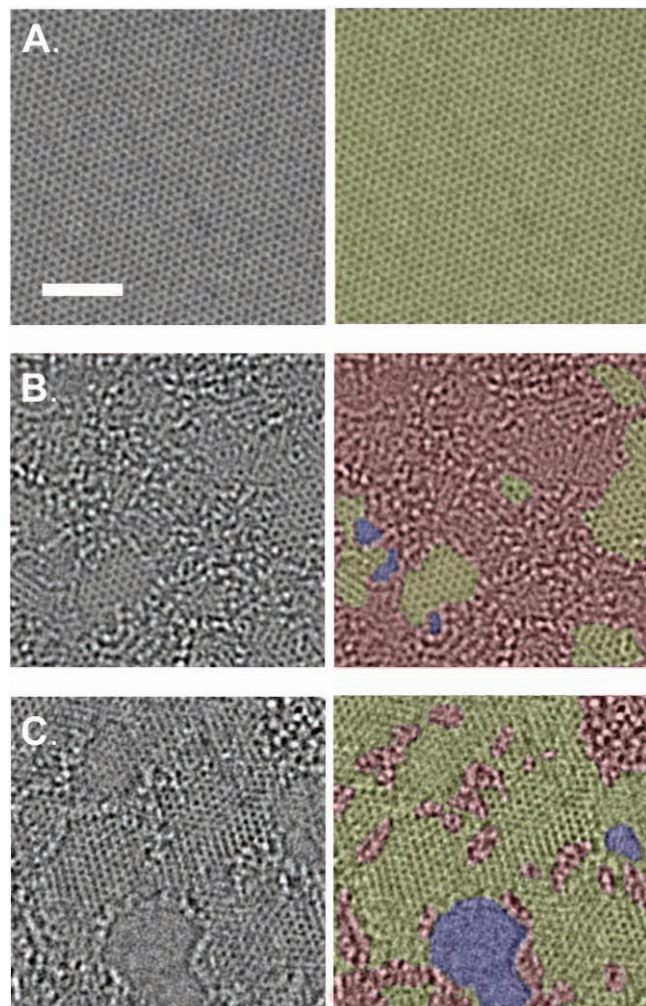
Figure 1. Aberration corrected TEM images of the following materials. Scale bar, denoting 2 nanometers, is valid for all images. (A) Single suspended sheet of graphene. On the right, graphitic area indicated in yellow. (B) Single suspended sheet of GO. On the right, holes are indicated in blue, graphitic areas in yellow, and high contrast, disordered regions, indicating oxygen functionalities, in red. (C) Suspended monolayer of raGO. On the right, holes indicated in blue, graphitic regions in yellow, and areas with remaining functionalities in red.

structure and 1.4 Å atomic spacing of graphene. The disordered, high contrast oxidized regions of the basal plane form a continuous network throughout the GO sheet.

Monolayer raGO (Figure 1C) is similarly structurally inhomogeneous with holes (blue), graphitic regions (yellow), and disordered areas with high contrast (red). The observed holes comprise approximately 5% of the area. An increase in the area of holes compared to GO is expected as CO and CO_2 form during annealing.[10] The anticipated significant increase in graphitic area observed, up to approximately 70% of the area, indicates a substantial restoration of the original sp^2 bonding character lost during the oxidation, by the reduction of oxygen functionalities. However, extensive disordered high contrast regions still exist, likely from nitrogen and oxygen functionalities which persist even after reduction and annealing.[8]

Uninterrupted translational order, as observed with pristine graphene, is not seen, being disrupted by the holes and the remaining functionalities.

This raGO material under study is substantially different from graphene as indicated by Figure 1. Although significantly restored graphitic nature is imparted upon reduction, the remaining functionalities and holes in raGO drastically differentiate it from graphene. Attempts at synthesizing limitedly oxidized graphene oxide or at introducing a carbon feedstock for the "healing" of raGO show promise for potentially addressing these observed differences between raGO and graphene, possibly resulting in minimal defects and reincorporation of carbon into the basal plane when missing from the synthesized raGO material.[6,11,22,23]

We turn now to a closer examination of the structure of GO. The main body of **Figure 2** shows another representative TEM image of GO, suitable for detailed examination. A high-contrast
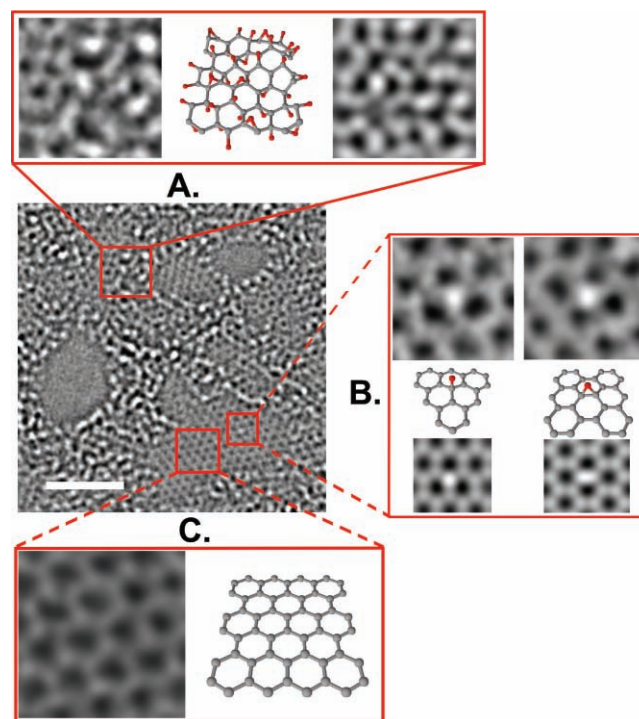
Figure 2. Aberration-corrected TEM image of a single sheet of suspended GO. The scale bar is 2 nm. Expansion (A) shows, from left to right, a 1 nm^2 enlarged oxidized region of the material, then a proposed possible atomic structure of this region with carbon atoms in gray and oxygen atoms in red, and finally the average of a simulated TEM image (see Supporting Information) of the proposed structure and a simulated TEM image of another structure where the position of oxidative functionalities has been changed. Expansion (B) focuses on the white spot on the graphitic region. This spot moved along the graphitic region, but stayed stationary for 3 frames (6 seconds) at a hydroxyl position (left portion of expansion (B)) and for 7 frames (14 seconds) at a (1,2) epoxy position (right portion of expansion (B)). The ball-and-stick figures below the microscopy images represent the proposed atomic structure for such functionalities. The simulated TEM image for the suggested structure (see Supporting Information) agrees well with the TEM data. Expansion (C) shows a 1 nm^2 graphitic portion from the exit plane wave reconstruction of a focal series of GO and the atomic structure of this region.

Materials
Views

www.MaterialsViews.com

ADVANCED
MATERIALS

www.advmat.de

COMMUNICATION

region is selected in Figure 2A. With this sample, adsorbates are understood to be limitedly present, and if present, to only be adsorbed onto the oxidized regions of GO. Grids heating prior to TEM imaging largely desorbs such weakly, physically bonded species. Furthermore, electron beam exposure induces desorption and motion of adsorbates,[18] resulting in minimally observed adsorbates in the similarly prepared and imaged graphene and raGO samples (Figure 1A and 1C). Finally, time-dependent changes in the overall area of the high contrast regions would be expected during TEM imaging if they were caused by large numbers of adsorbates as some of these adsorbates would desorb under electron beam exposure. However, the increased Van der Waals interaction between adsorbates and oxidative functionalities compared to their interaction with graphitic regions means that any remaining adsorbates would be adsorbed to the oxidized regions of GO. High contrast regions are thus primarily from oxidized carbons and limitedly from adsorbates, which indicate an underlying oxidized region. The high amount of contrast variation indicates a high density of oxygen functionalities, with each carbon likely being oxidized with no order between functionalities.

In the high contrast regions, oxygen atoms are present in a much higher density and greater numbers will be mobilized by the electron beam. After studying the times series (see Supporting Information Video S1), although cases of functionalities being stable for multiple seconds can be found, most functionalities seem to be mobile of the timescale of a second. Given this, significant changes in the bonding can occur over the course of each captured frame, and each micrograph could represent multiple bonding configurations between the carbon basal plane and oxidative functionalities. Figure 2A shows such a region with a high degree of oxidative functionalities. A possible representative local atomic structure for this oxidized region is proposed, but of course the complicated contrast within this region makes any specific definition of a structure for this region impractical. Simulations of TEM images were made from this proposed structure and another structure where the location of the oxidative functionalities was changed, the average of which is compared to the obtained micrograph.

Figure 2B highlights a mostly graphitic region with isolated anomalous bright spots. The anomalies are dynamic (on the timescale of a second, see Supporting Information Video S1), likely indicating isolated mobile oxygen functionalities. The anomalies of Figure 2B are consistent with simulations of TEM images (see Supporting Information) for an oxygen resting at a hydroxyl position (left), or an oxygen resting at an (1,2) epoxy position (right). Multiple instances of such isolated functionalities are observed in GO. Although it is possible that the observed adatoms were carbon adatoms, the likelihood of mobilizing a carbon bound to the graphitic sheet or even from a nearby hole is unlikely given the multiple bonds required to be broken (with a graphene C-C bond energy of 4.9 eV)[24] compared to those required to be broken to mobilize an oxygen from common functionalities expected in GO: 2.1 eV for (1,2) epoxies and 0.7 eV for hydroxyls.[25]

The mobility of these functionalities is a consequence of the incident 80 keV electron bombardment, which transfers a maximum of 11.8 eV to an oxygen atom,[26] well over epoxy and hydroxyl bond energies and well over the hopping barrier,

being much lower.[27] Electron beam induced bond breakage occurs, mobilizing atoms which rest at stable positions nearby on the basal plane. The energy for the ejection of an atom from the sheet is much greater.[28] For GO we observe minimal loss of high contrast and stable hole size indicating relatively little overall beam-induced oxygen- or carbon-ejection, respectively.

Figure 2C highlights a graphitic region of GO. The sharpened blowup was obtained from the exit plane wave reconstructed from a 12-member focal series (for details see Supporting Information and Figure S3). The highly graphitic nature of this region is striking. Some bond strain does occur at the interface of oxidized and unoxidized regions, but the interior of the graphitic regions, when lacking oxygen functionalities, are found to be largely unaffected by this strain. The different graphitic regions can be thought of as flakes of nearly pure graphene separated by highly oxidized and thus structurally modified regions. The graphitic domains are mis-tilted in the azimuthal direction with respect to each other. This combined with bond strain at the interface of the graphitic and oxidized regions results in the observed blurring of diffraction spots compared to graphene[29] (see Supporting Information Figure S1).

We now examine the raGO material under study in detail. **Figure 3** shows a representative image, similar to that presented in Figure 1C. A significant portion of raGO is indeed graphitic, but certainly raGO cannot be properly characterized as constituting "graphene". The examined raGO material was found to be overall highly sensitive to electron beam induced degradation to the point that meaningful exit plane wave reconstruction was not possible. This indicates a higher instability of raGO, as compared to graphene, or even to GO (we found, however, a significantly higher stability for *bilayer* raGO, as compared to *monolayer* raGO, as discussed below).

Nevertheless, the high amount of restored graphitic area in raGO supports the supposition that the parent GO contains mostly hydroxyl and epoxy functionalities. Only these oxidative functionalities (other than high energy peroxide functionalities) would result in fully restored graphitic character once reduced, as other functionalities would induce C-C bond breakage.[29]

Figure 3A highlights regions of raGO with high contrast spots, likely representing remaining functional groups. These are understood to be either oxygen functionalities from the initial oxidation or nitrogen functionalities from the hydrazine reduction.[8] Although specific determination of a structure can not be made, a likely structure for this region is proposed in Figure 3A. A simulated TEM image for the proposed structure is included for comparison. Figure 3B highlights a fully restored graphitic region of raGO.

It is instructive to examine in some detail the relative temporal stability of graphene, GO, and raGO when exposed to the agitation of the imaging TEM electron beam. Under our imaging conditions, graphene is exceptionally stable, suffering only occasional knock-on damage.[28] **Figure 4** contrasts time series images of GO and raGO. GO was seen to be stable under the beam with each of the discussed regions not changing in area percentage during the obtained time series (75 seconds) (Figure 4A). This indicates that although atoms may become mobile within the GO plane under electron beam irradiation, significant atom ejection does not occur, which would result in changes to these percentages, indicating degradation of the
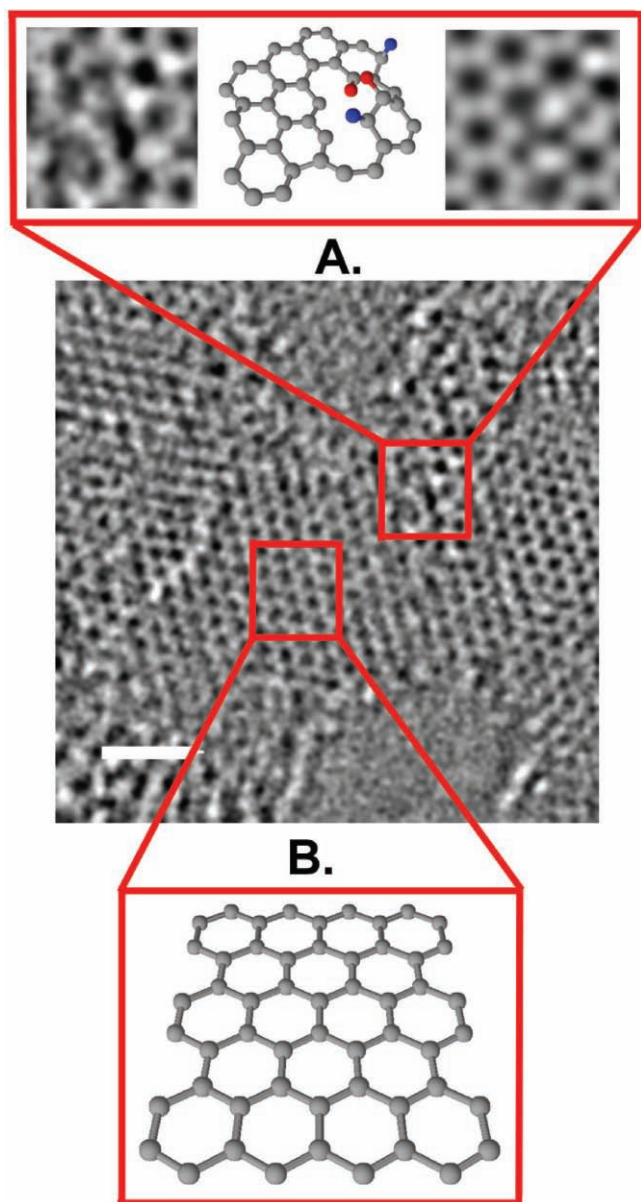
Figure 3. Aberration-corrected TEM image of a monolayer of raGO. The scale bar is 1 nm. Expansion (A) shows, from left to right, an enlarged region of the micrograph, then a proposed possible structure for the region where oxygen (indicated in red) and nitrogen (blue) remain as functionalities on the sheets, and finally a simulated TEM image for this proposed structure. Expansion (B) shows the structure of a graphitic region.

Figure 4. Aberration-corrected TEM images of (A) GO and (B) raGO from acquired time series. Scale bar, indicating 2 nm, is valid for all images. Frames show the two materials at the indicated number of seconds. GO is seen to be overall stable with its regions changing morphology, but not overall area. raGO is seen to degrade significantly over the course of the obtained time series.

material. As discussed previously, mobile oxygen functionalities result in the shift of boundaries between the graphitic and oxidized regions as functionalities move along the basal plane. The effective motion of functionalities does not result in an averaging of these functionalities across the GO sheet, indicating mainly sp^2 or sp^3 bonding character for the most stable regions, as expected from geometrical constraints and aromaticity. It was noticed in the acquired videos that small holes (<1 nm^2 in area) which were present during the beginning of the obtained time series seemed to be closed over the course of the time series. This observation supports the notion that if a carbonaceous feedstock (in this case mobilized carbon or carbon from the limited adsorbates) is present, carbon lost from the basal plane, occuring during the synthesis of GO, could possibly be reincorporated into the sheet under the proper experimental conditions. A video of the progression of GO under the electron beam can be found online (see Supporting Information Video S1).

The dynamics of raGO under the electron beam indicate significant degradation over relatively short time periods (Figure 4B). Degradation revolves around highly active regions with limited connectivity to the main raGO sheet, making them more easily accelerated under the electron beam (very noticeable in Supporting Information Video S2). Bi-layer raGO shows increased stability under the electron beam, though it, too, degrades more quickly than GO or graphene (Supporting Information Figure S2 and Video S3).

Contrasting the presented images of GO and raGO further substantiates that, from the various oxygen functionalities that have been proposed to exist in GO,[4] the main functionalities are indeed hydroxyls and (1,2) epoxies, and that carbonyls form mainly around the holes in the sheet. This is evidenced by the observed stability of hydroxyls and (1,2) epoxies and the significantly restored graphitic nature of raGO, the restoration being

possible only when these functionalities are dominant. Also, since bond breakage associated with carbonyl formation likely accommodates hole formation and expansion,[30] and substantial XPS data indicates the presence of these groups,[8] carbonyls likely form at the edges of the observed holes within the GO sheet.

Our experiments greatly elucidate the important and previously unknown structure of GO. Previous attempts at experimentally determining this structure involved analyzing chemical reactivity, XPS, Raman, NMR, IR, conductivity, TGA, diffraction and absorption,[4] were relevant only to macro to microscopic regions of GO. Theoretical calculations have conversely been limited to considering regions less than 100 atoms,[19] sometimes less than 10 atoms,[25] in extent, and then generalizing a larger structure. Since regions larger than 100 atoms exist with only sp^2 or sp^3 bonding nature, these theoretical considerations are seen to poorly describe GO. Likewise, when bulk properties are generalized down to determine the most likely atomically defined structure, many nuances are overlooked. For instance, XPS results indicating carbonyls within GO have been attributed to these groups being along the microscopic edges of GO. The observation of holes, likely with edge carbonyls, every few nanometers redefines how these results should be interpreted.

Our observations and deductions about the structure of GO can be summarized as follows. **1.** Graphitic regions up to 8 nm^2 remain. **2.** Oxidized regions exhibit no order with regards to oxidation, have minimal sp^2 bonding character, and form a continuous network across the GO sheet. **3.** Holes are present, usually under 5 nm^2. **4.** Hydroxyls and (1,2) epoxies are the dominant functionalities. Carbonyls likely exist along the edges of the holes. **5.** Largely unstrained sp^2 bonds exist between carbons within the core of graphitic regions. **6.** Lines of graphitic or oxidized regions do not form and no superstructures are formed.

Given these deductions, theories of the structure of GO can be evaluated. Proposals for ordered functional groups or long range order, for instance lines of aromatic regions[4] or lines of oxidized regions[4,27] are unsubstantiated. Predictions of densely oxidized regions with hydroxyls and (1,2) epoxies as the primary functionalities and carbonyls along the edges are supported,[19,29,31–33] whereas prediction of (1,3) epoxies,[34] carbonyls as dominant functionalities,[4] other functionalities,[35] numerous isolated functionalities,[35] or just epoxies[36] are not supported. Theories disregarding significant aromaticity[19] are likewise not supported. Theoretical considerations of less than 10 carbons[25] in GO are discarded owing to the high degree of structural inhomogeneity. Also, the proposed mechanism of "unzipping" GO sheets caused by sequential epoxies[27] is not observed. Adjacent functionalities with positions indicative of epoxies are observed, but continuation of this defect line is not; thus the proposed microscopic cleavage of GO sheets via this mechanism is doubtful.

Given all these considerations, the structure proposed by Lerf[33] is supported, albeit with modifications. The sizes of graphitic and oxidized regions are much larger than those proposed by Lerf and with this studied GO material, holes are found throughout the sheet.

Supporting Information

Supporting Information is available from the Wiley Online Library or from the author.

Acknowledgements

[1] X. Li, Y. Zhu, W. Cai, M. Borysiak, B. Han, D. Chen, R. D. Piner, L. Colombo, R. S. Ruoff, *Nano Lett.* **2009**, *9*, 4359.

[2] S. Park, R. S. Ruoff, *Nat. Nanotechnol.* **2009**, *4*, 217.

[3] C. Berger, Z. Song, X. Li, X. Wu, N. Brown, C. Naud, D. Mayou, T. Li, J. Hass, A. N. Marchenkov, E. H. Conrad, P. N. First, W. A. de Heer, *Science* **2006**, *312*, 1191.

[4] T. Szabo, O. Berkesi, P. Forgo, K. Josepovits, Y. Sanakis, D. Petridis, I. Dekany, *Chem. Mater.* **2006**, *18*, 2740.

[5] A. Sinitskii, D. V. Kosynkin, A. Dimiev, J. M. Tour, *ACS Nano* **2010**, *4*, 3095.

[6] Q. Su, S. Pang, V. Alijani, C. Li, X. Feng, K. Müllen, *Adv. Mater.* **2009**, *21*, 3191.

[7] G. Eda, G. Fanchini, M. Chhowalla, *Nat. Nanotechnol.* **2008**, *3*, 270.

[8] H. A. Becerril, J. Mao, Z. Liu, R. M. Stoltenberg, Z. Bao, Y. Chen, *ACS Nano* **2008**, *2*, 463.

[9] H. Chen, M. B. Müller, K. J. Gilmore, G. G. Wallace, D. Li, *Adv. Mater.* **2008**, *20*, 3557.

[10] I. Jung, D. Dikin, S. Park, W. Cai, S. L. Mielke, R. S. Ruoff, *J. Phys. Chem. C* **2008**, *112*, 20264.

[11] Y. Liang, J. Frisch, L. Zhi, H. Norouzi-Arasi, X. Feng, J. P. Rabe, N. Koch, K. Mullen, *Nanotechnology* **2009**, 434007.

[12] J. C. Meyer, C. O. Girit, M. F. Crommie, A. Zettl, *Appli. Phys. Lett.* **2008**, *92*, 123110.

[13] W. S. Hummers, R. E. Offeman, *J. Am. Chem. Soc.* **1958**, *80*, 1339.

[14] N. R. Wilson, P. A. Pandey, R. Beanland, R. J. Young, I. A. Kinloch, L. Gong, Z. Liu, K. Suenaga, J. P. Rourke, S. J. York, J. Sloan, *ACS Nano* **2009**, *3*, 2547.

[15] J. C. Meyer, A. K. Geim, M. I. Katsnelson, K. S. Novoselov, D. Obergfell, S. Roth, C. Girit, A. Zettl, *Solid State Commun.* **2007**, *143*, 101.

[16] J. C. Meyer, C. Kisielowski, R. Erni, M. D. Rossell, M. F. Crommie, A. Zettl, *Nano Lett.* **2008**, *8*, 3582.

[17] M. D. Rossell, R. Erni, M. Asta, V. Radmilovic, U. Dahmen, *Phys. Rev. B* **2009**, *80*, 024110.

[18] J. C. Meyer, C. O. Girit, M. F. Crommie, A. Zettl, *Nature* **2008**, *454*, 319.

[19] J. T. Paci, T. Belytschko, G. C. Schatz, *J. Phys. Chem. C* **2007**, *111*, 18099.

[20] R. S. Pantelic, J. C. Meyer, U. Kaiser, W. Baumeister, J. M. Plitzko, *J. Struct. Biol.* **2010**, *170*, 152.

[21] C. Gomez-Navarro, J. C. Meyer, R. S. Sundaram, A. Chuvilin, S. Kurasch, M. Burghard, K. Kern, U. Kaiser, *Nano Lett.* **2010**, *10*, 1144.

[22] X. Li, G. Zhang, X. Bai, X. Sun, X. Wang, E. Wang, H. Dai, *Nat. Nanotechnol.* **2008**, *3*, 538.

[23] V. López, R. S. Sundaram, C. Gómez-Navarro, D. Olea, M. Burghard, J. Gómez-Herrero, F. Zamora, K. Kern, *Adv. Mater.* **2009**, *21*, 4683.

[24] D. W. Brenner, O. A. Shenderova, J. A. Harrison, S. J. Stuart, B. Ni, S. B. Sinnott, *J. Phys.: Cond. Matter* **2002**, *4*, 783.

[25] R. J. W. E. Lahaye, H. K. Jeong, C. Y. Park, Y. H. Lee, *Phys. Rev. B* **2009**, *79*, 125435.

[26] R. F. Egerton, F. Wang, P. A. Crozier, *Microscopy Microanal.* **2006**, *12*, 65.

[27] J.-L. Li, K. N. Kudin, M. J. McAllister, R. K. Prud'homme, I. A. Aksay, R. Car, *Phys. Rev. Lett.* **2006**, *96*, 176101.

[28] C. O. Girit, J. C. Meyer, R. Erni, M. D. Rossell, C. Kisielowski, L. Yang, C. H. Park, M. F. Crommie, M. L. Cohen, S. G. Louie, A. Zettl, *Science* **2009**, *323*, 1705.

[29] H.-K. Jeong, Y. P. Lee, R. J. W. E. Lahaye, M.-H. Park, K. H. An, I. J. Kim, C.-W. Yang, C. Y. Park, R. S. Ruoff, Y. H. Lee, *J. Am. Chem. Soc.* **2008**, *130*, 1362.

[30] R. Backreedy, J. M. Jones, M. Pourkashanian, A. Williams, *Faraday Discussions* **2002**, *119*, 385.

[31] M. C. Kim, G. S. Hwang, R. S. Ruoff, *J. Chem. Phys.* **2009**, *131*, 064704.

[32] W. Cai, R. D. Piner, F. J. Stadermann, S. Park, M. A. Shaibat, Y. Ishii, D. Yang, A. Velamakanni, S. J. An, M. Stoller, J. An, D. Chen, R. S. Ruoff, *Science* **2008**, *321*, 1815.

[33] A. Lerf, H. He, M. Forster, J. Klinowski, *J. Phys. Chem. B* **1998**, *102*, 4477.

[34] M. Mermoux, Y. Chabre, A. Rousseau, *Carbon* **1991**, *29*, 469.

[35] W. Scholz, H. P. Boehm, *Z. Anorg. Allgem. Chemie* **1969**, *369*, 327.

[36] U. Hofmann, R. Holst, *Berichte der Deutschen Chemischen Gesellschaft* **1939**, *72*, 754.